International Journal of Biomass Utilization and Sustainable Energy
Volume 2, 2024 [54-65]

Properties of poly(butylene adipate-co-terephthalate)/thermoplastic starch filled with treated and untreated sugarcane bagasse fiber

Maisara Azad Mat Akhir[1,2*], Syazana Ahmad Zubir[1] and Mariatti Jaafar[1]

[1] *School of Materials and Mineral Resources Engineering, Universiti Sains Malaysia, 14300 Nibong Tebal, Pulau Pinang, Malaysia*

[2] *Faculty of Chemical Engineering & Technology, Universiti Malaysia Perlis (UniMAP), 02600 Arau, Perlis, Malaysia*

ABSTRACT

Sugarcane bagasse, comprising fibrous rind and spongy pith, is frequently employed as a reinforcing agent in both concrete and plastic composites. In thin plastic films, sugarcane bagasse is typically utilized as finely ground particles within the composite film. The integration of this agricultural byproduct into biodegradable plastic films could potentially lower production expenses and promote the film's biodegradability. This study presents the development of poly(butylene adipate-co-terephthalate) (PBAT)/thermoplastic starch (TPS) (90/10) formulations incorporating varying loadings of sugarcane bagasse fibers. The impact of alkaline and silane surface treatments on tensile strength, thermal properties, and water barrier properties was investigated. Upon the inclusion of sugarcane bagasse (5%, 10%, 15%, and 20%), a decrease in tensile strength from 23.47 to 8.41 MPa and elongation at break from 1135% to 55.83% was observed. Conversely, the Young's modulus increased from 47.12 to 188.50 MPa following the addition of 20% sugarcane bagasse in the PBAT/TPS matrix. Modest enhancements in tensile properties, thermal characteristics, and water barrier properties were noted after treating the bagasse fibers with alkaline and silane. Scanning Electron Microscope (SEM) analysis revealed that silane-treated sugarcane bagasse exhibited increased surface roughness due to the removal of lignin and hemicellulose, facilitating better adhesion between the fibers and the PBAT/TPS matrix.

Keywords: Fiber composites, PBAT, tapioca starch, polymer blend, sugarcane bagasse

1. INTRODUCTION

Increasing consumer awareness on reducing waste and environmental pollution from conventional non-biodegradable plastic led researchers to study the utilization of plant-based agricultural residues into polymer composite formulation. Employing this agricultural waste from the industry as reinforcement and filler materials in the biodegradable plastic formulation can improve the plastic stiffness, apart from their high biodegradability, availability, eco-friendly, renewability, lightweight alternative materials, and cheaper cost of raw material. There are many opportunities to convert the agricultural residues such as sugarcane bagasse, empty fruit bunch, and fruit peels from industries and convert them into wealth.

Sugarcane bagasse is one of the most produced wastes derived from sugar and liquor productions. Its stalk is composed of strong and fine long fibrous outer layer (rind) and short, soft, and spongy structured inner part (pith), which mainly consists of sucrose (Lee & Mariatti, 2008). The rind part exhibits a higher tensile strength of 8.68 MPa, Young's modulus of 2 GPa, and

---

[*] Corresponding author: maisaraazad@unimap.edu.my

elongation at break of 4.24% compared to the pith part, which are 2.19 MPa, 1.2 GPa and 1.82 %, respectively (Jamali et al., 2021). Previous studies reported that the rind composites exhibited superior strength and stiffness in comparison with the pith composites (Lee & Mariatti, 2008; Wirawan et al., 2011). Due to its availability, relatively high mechanical properties, low cost and large volume of residue, sugarcane bagasse can be an ideal material to be reinforced into the biocomposite formulation. Such fibrous sources can be combined with polymers to form polymer matrix composites in various forms, including woven mats, chopped fibers, and powders.

However, the utilization of natural fibers in the polymer-matrix composite is limited by their hydrophilic characteristic, high moisture absorption level, weak fiber dispersion into the matrix, poor wettability and interfacial adhesion with a hydrophobic polymer. Fiber agglomeration tends to occur during melt blending, which causes debonding and further weakens the mechanical and thermal properties. The bagasse fiber contains about 45-55% cellulose, 20–25% hemicellulose, 18–24% lignin, 1.3% ash, and 2.8% other components (Ramlee et al., 2019). The highly crystalline and tightly packed cellulose fibers account for good chemical and mechanical properties. On the other hand, the lignin that binds the hemicellulose and cellulose by ester linkages and hydrogen bonds, respectively, are the layers that hinder their interaction with the matrix. Thus, the removal of lignin, hemicellulose and other components can contribute to a high specific property of the composite. Moreover, physical and chemical treatment, such as surface modification using coupling agents can improve fiber-matrix interfacial adhesion. Chemically treated natural fibers have the potential to be less hydrophilic and have a better bonding with the matrix. To improve interfacial strength, silane coupling agents are frequently used in polymer composites.

Poly(butylene Adipate Terephthalate) (PBAT) blended with thermoplastic starch (TPS) had been studied by a number of researchers due to its competitive mechanical properties, good thermal stability and barrier properties, good biodegradability, eco-friendly, safe for food packaging, and affordable price range. PBAT/TPS blend had been used as matrix reinforced with natural fibers such as oat hulls (Cardoso et al., 2018), rice husk (Yap et al., 2020), babassu mesocarp (De Moura et al., 2021; Nunes et al., 2018) and jute fiber (Yokesahachart et al., 2021). However, to the best of our knowledge, the incorporation of sugarcane bagasse fiber in PBAT/TPS blend had been rarely studied. Furthermore, limited study had been done on the effect of silane-treated bagasse on PBAT/TPS blend. Since both TPS and bagasse are hydrophilic in nature, the amount of these components is critical to ensure good barrier properties of the composite's film. Thus, this paper investigates the effect of different sugarcane bagasse fiber loadings on PBAT/TPS (90/10) matrix and surface modification treatment with alkaline and GPTMS silane on the tensile, thermal, morphology and water barrier properties. The PBAT/TPS (90/10) blend ratio was chosen as the composite matrix due to its high tensile properties and good barrier properties, meeting the requirements for mulch application.

2. MATERIALS AND METHODS

2.1 Materials

Sugarcane bagasse was supplied from a nearby local market. The outer layer of sugarcane bagasse (rind) was separated from the inner layer of sugarcane bagasse (pith). Rind parts were immersed in deionized water for 24 hr at ambient temperature, and then washed with water to remove soluble sugars and impurities. After washing, the sugarcane bagasse was dried in the oven at 70 ^{0}C for 24 hrs, and then ground and sieved to remove coarse fibers.

PBAT (Grade Ecoflex F Blend C1200, BASF, USA) supplied by Innovative Pultrusion Sdn Bhd, Negeri Sembilan, Malaysia was used as a blend component and matrix. Modified tapioca starch was bought from Thye Huat Chan Sdn Bhd (Penang, Malaysia). Glycerol (85 % purity), 3-Glycidoxypropyl trimethoxysilane, sodium hydroxide, and acetic acid were purchased from Sigma-Aldrich Sdn. Bhd., Malaysia.

2.2 Fiber treatment

For treated sugarcane bagasse (SB), SB powder was soaked in 8 w/v% of NaOH mixed with distilled water for 2 hrs to remove lignin and hemicellulose. When the SB was dispersed, the pH of the mixture was adjusted to 7 using acetic acid. The SB powder was filtered and rinsed several times with distilled water, and dried in the oven at 70ºC for 24hrs. A mixture of ethanol and deionized water (6:4) was prepared, and GPTMS (6% wt./wt.) was added dropwise and stirred. The mixture were adjusted until pH 4 using acetic acid, and the alkaline treated SB powder were further soaked in the solution for 2 hrs. The silane-treated SB (SBT) were filtered and dried in an oven for 24 hrs.

2.3 Blend and composite preparation

Blends were created through melt-mixing using a torque rheometer. Tapioca starch and PBAT were dried at 70°C overnight prior to use to prevent excessive hydrolysis. Starch and glycerol at a ratio of 70/30 wt% were dry-mixed in the Haake internal mixer for 5 minutes at a speed of 40 rpm. Subsequently, blends of PBAT with 10 wt% plasticized starch were prepared in the internal mixer at a temperature of 160°C with a rotor speed of 50 rpm for 15 minutes. For composite preparation, both silane-treated and untreated SB fibers at 5%, 10%, 15%, and 20% wt% were manually premixed with PBAT and TPS prior to the compounding process. The samples were then compression molded at a temperature of 160°C: 5 minutes for preheating, 5 minutes for heat compression, and 3 minutes for cooling, following ASTM D638 Type IV specifications, with a thickness of 1 mm for tensile testing.

2.4 Characterization analysis

The tensile properties of the composites were assessed using an INSTRON Universal Testing Machine in accordance with the ASTM D638 standards. The initial grip separation was established at a 30 mm gauge length, while the cross-head speed was set at 50 mm/min, utilizing a 5 kN load cell at room temperature. Parameters evaluated included maximum tensile strength (MPa), Young's modulus, and elongation at break (%). Each composite combination underwent seven tests.

The morphology of PBAT/starch (90/10) blend and reinforced SB fiber composite were obtained using an ultra high resolution - scanning electron microscope (SEM) (Hitachi-Regulus, Japan). The cryo-fractured samples were coated with a thin layer of titanium and the micrographs were recorded under magnification of 200x at 3kV.

The thermal stability of the blend and composites were analyzed using thermal gravimetric analysis (TGA) (Pyris 6, PerkinElmer, USA). Approximately 18 mg of sample was used, and the tests were performed from room temperature to 600 °C under nitrogen atmosphere with a heating rate of 20°C/min.

The water absorption test followed ASTM D570 standards, employing square samples measuring 20 x 20 x 3mm for each composite. Before testing, samples were dried at 50°C until reaching a constant weight (W_i), then cooled to room temperature in a desiccator. Subsequently, each composite was submerged in distilled water for 72 hours, removed, gently dried with tissue paper, and weighed (W_f). The water absorption percentage was determined using Equation (1).

$$\text{Water absorption percentage (\%)} = \frac{W_f - W_i}{W_i} \times 100\% \qquad (1)$$

The hydrophobicity of the composite film was assessed using water contact angle analysis. Samples were cut to fit the sample stages of a contact angle goniometer (Lux, DSA100, Germany). A precise syringe deposited a droplet of distilled water onto the film's surface, and the contact angle was measured using a CCD camera and analyzed with an image processing video card. The angle between the tangent and the baseline at the droplet boundary was automatically calculated, with each set of samples measured ten times and averaged for the results.

The chemical structures of the PBAT/TPS (90/10) blend and various fiber-loaded composites were analyzed using a FT-IR spectrometer (Perkin Elmer, USA) equipped with diamond attenuated total reflectance (ATR) techniques. Spectral bands were recorded as an average of 32 scans within the range of 4000 to 500 cm^{-1}.

3. RESULTS AND DISCUSSION

3.1 Tensile properties

Figure 1 shows the tensile properties of the PBAT/TPS blend and composites.

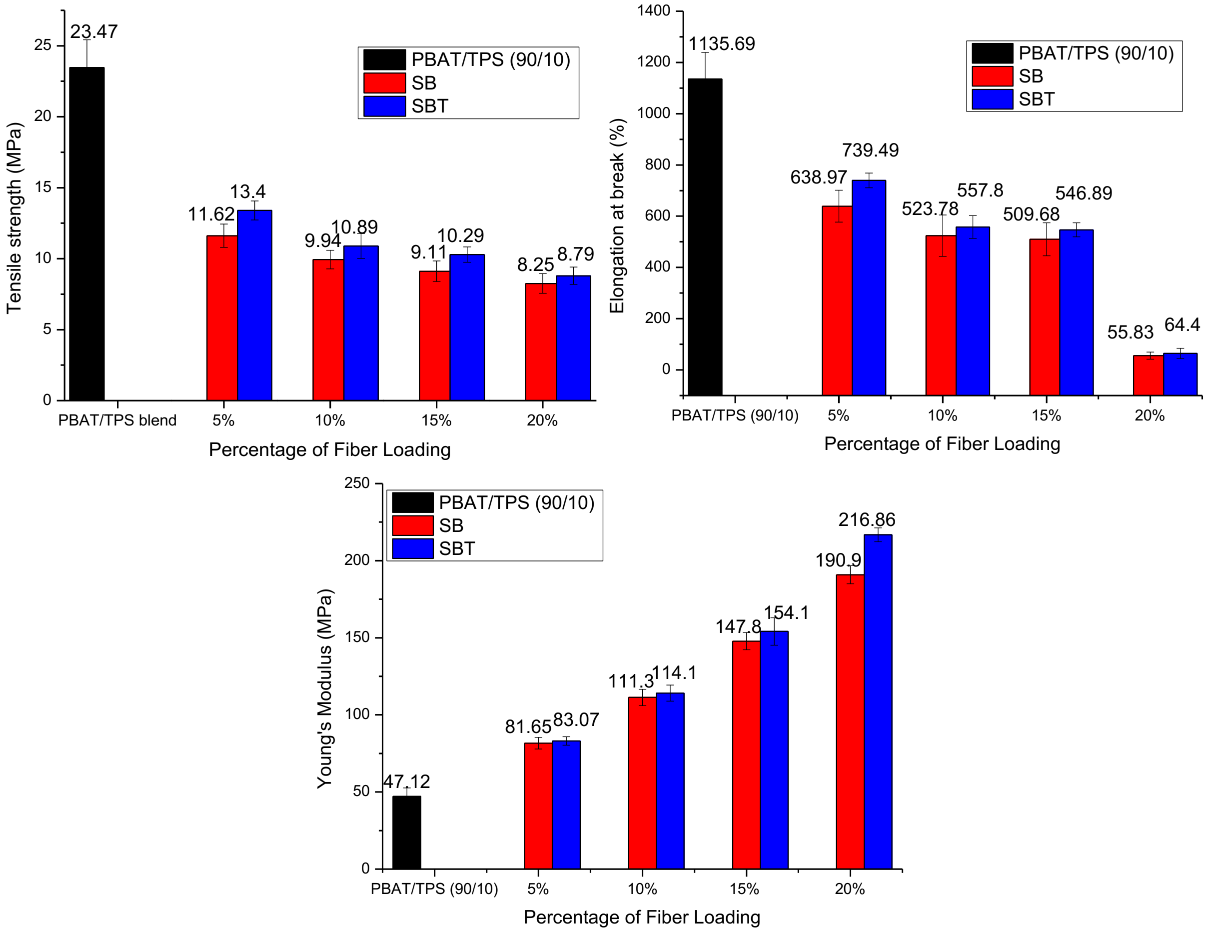

Figure 1: Tensile strength, elongation at break and Young's modulus of PBAT/TPS (90/10) reinforced with 5, 10, 15, and 20% of fiber (SB=sugarcane bagasse without treatment; SBT= Treated sugarcane bagasse)

There was a significant reduction in tensile strength from 23.47 to 7.94MPa, and film flexibility from 1135.69 to 55.83% with the addition of SB fiber. The elongation at break of PBAT/TPS/SB composites decreased with increasing SB weight percentage due to reduced chain mobility and increased film's brittleness. Increasing the fiber fraction in the composites will decrease the amount of available PBAT for elongation, and thus lead to brittle composite film. Furthermore, the effects of silane surface treatment were more notable when 5% of SBT powder was incorporated in PBAT/TPS matrix with an improvement about 15% in tensile strength and elongation at break. This infers that the fibers had enhanced their stress transfer ability due to better interfacial bonding between the hydrophilic fibers, silane coupling agent, and hydrophobic matrix, which can be observed by SEM image in Figure 2(d). However, after the addition of SB and SBT powder with 5% to 15% loading, there were not huge means differences in tensile strength and elongation at break with a range of 13.4 to 9.11 MPa and 739.49 to 509.68%, respectively. However, composite with 20% fiber loading showed a remarkable reduction in fiber's flexibility and strength as it dropped to 55.83 and 64.41%

and tensile strength of 8.25 and 8.79 MPa for both untreated and treated fibers, respectively. This might be attributed to the action of fibers acting as flaws at higher filler fraction (Chen et al., 2015). Composite with a higher amount of filler tend to agglomerate, and a limited amount of PBAT/TPS matrix to wrap the fibers has resulted in poor transmission of stress from matrix to fiber. Additionally, lower tensile properties of SBT 20% composite could be related to insufficient GPTMS silane coupling agent to provide adequate reinforcement effect to the fiber matrix interface for higher filler concentrations.

Figure 1 also implies that the SB fiber acted as a filler rather than as reinforcement since the film strength and ductility decreased after SB addition. Nevertheless, the film's toughness and stiffness were greatly enhanced from 47.12 to 216.86 MPa as specified in Young's modulus values with increasing fiber volume from 0% to 20%. The addition of SB fibers resulted in higher rigidity and hardness values of the composites compared to their matrix counterpart. It may be due to increasing SB fiber resulted in increasing cellulose content which accounts for the stiffness property of the natural fiber. Silane-treated SB filler had a slight improvement in stiffness compared to untreated SB. This increment could be explained by the improved adhesion between cellulosic fiber and polymeric matrix due to the removal of the waxy and grassy layer from the SB fiber surface via alkaline treatment, as well as the reduced hydrophilicity via GPTMS silane treatment. Even though the addition of SB fibers led to a reduction in tensile strength and elongation at break, it greatly enhanced the material's stiffness and lowered the material cost.

3.2 Morphological analysis

Figure 2 illustrates the SEM images of PBAT/TPS (90/10) blend, the highest (20%) and lowest (5%) loadings of SB fibers. Figure 2 (b) and (e) show the distribution of SB fiber in PBAT/TPS matrix before starch particle removal. In contrast, Figure 2 (a), (c & d) and (f & g) are the enlarged images of composites corresponding to 0%, 5%, and 20% of SB fibers, respectively. After starch domain extraction, well distributed circle voids can clearly be observed in the PBAT matrix. Referring to the SEM images, the incorporation of SB fibers destroyed the surface integrity of the PBAT/TPS matrix. This could be related to the reduction of approximately half of the tensile strength and elongation at break of the composite compared to PBAT/TPS matrix. Moreover, increasing fiber contents lead to rougher and higher surface porosity, as can be correlated with stronger and enhanced film ductility of the composites with lower fiber contents than higher fiber contents.

From Figure 2 (b & c) and (e & f), the fiber pull-out and fiber breakage in the composite samples without treatment can be seen. Furthermore, numerous gaps between the bagasse fiber and the PBAT/TPS matrix can be observed, indicating a poor interfacial adhesion between the fiber and matrix interfaces. Unlike untreated SB fiber, the surface structures of the treated SB fiber (Figure 2 (d) & (g)) displayed rougher surfaces with lesser spongy voids within the fiber. This is due to the removal of some of the hemicelluloses, lignin, pectin and wax components in the bagasse fiber, which is favorable for reinforcement effect and water barrier property compared to untreated bagasse. On the other hand, the absence of fiber pull-out and reduction in gaps present in the 5% SBT composites with surface modification by alkaline and silane coupling treatment in Figure 2(d) indicated better fiber-matrix affinity and good adhesion. This is due to the fact that the addition of GPTMS can form a good siloxane network, resulting in a high tensile strength due to strong chemical interaction between the matrix and SB fibers via the presence of a cross-linked network of silane groups (Kane et al., 2016). Similar observations of silane-treated composites have been reported by Cordeiro et al. (2017) and Pereira da Silva et al. (2017), showing that GPTMS silane coupling agents improved the compatibility between the polymer matrix and fiber.

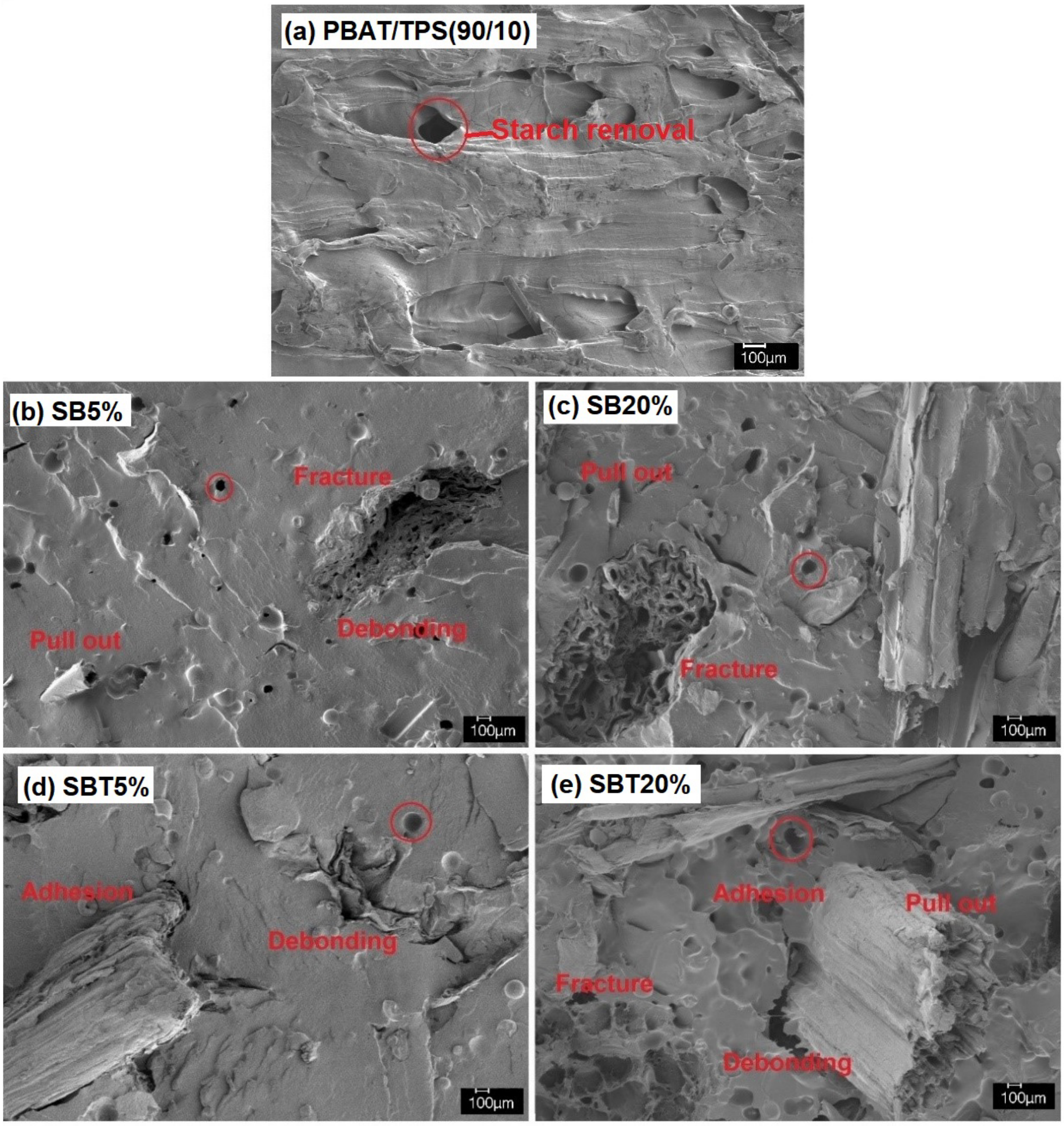

Figure 2. SEM images of PBAT/TPS (90/10) with treated and untreated SB.

However, the appearance of a distinct debonding gap between bagasse fiber and matrix with fiber pull-out can be observed in SBT 20% composites (Figure 2(e)). This might be due to inadequate silanization by GPTMS coupling agent to cover fiber's surface with organofunctional alkoxysilane molecules at a higher amount of fiber loading, which results in weak fiber and matrix interaction (Kane et al., 2016). The SEM image of 20% SBT fibers agreed with the finding in tensile testing, which reveals that higher fiber volume causes significant decrement in tensile strength and elongation at break.

3.3 Thermal stability analysis

TGA was performed to investigate the film's limiting temperature and the influence of fiber treatment on the thermal stability of the composites. Figure 3 shows the TG and derivative thermograms (DTG) curves. From the graphs, it can be seen that there are two main zones of weight loss; one in the range of 280 to 360 °C and one between approximately 380 and 460 °C. Pure PBAT matrix is a thermally stable polymer that begins to degrade near 370 °C with high degradation rates at temperature 425 °C. Whereas PBAT/TPS (90/10) blend experienced two steps of decomposition at ~360 and 424.4 °C, representing the elimination of amylose and amylopectin components from starch, and PBAT, respectively. However, the peak at 50–250 °C, which indicates the elimination of glycerol and water as specified by previous studies (González Seligra et al., 2016; Lendvai et al., 2017; Liu et al., 2019), was not clearly observed in the TGA and DTG curves. This is probably due to

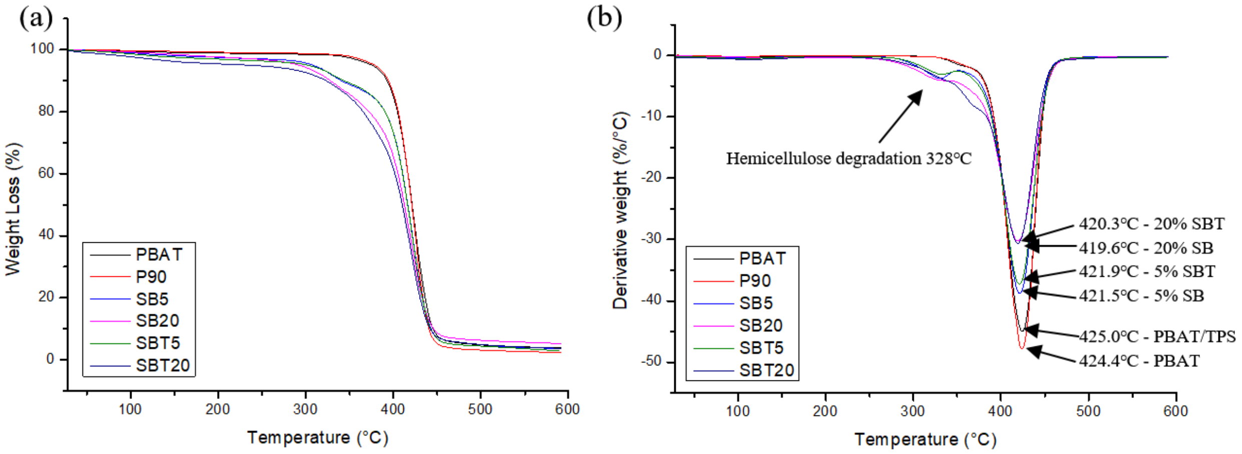

Figure 3: (a) TGA and (b) DTG of treated and untreated PBAT/TPS/SB composites.

the relatively small amount of glycerol (30%) in TPS fraction inside the PBAT/TPS (90/10) blend.

Furthermore, the weight losses at 400 °C of the pure PBAT, PBAT/TPS (90/10), and composite films with 5 and 20% treated and untreated fibers were about 95.9, 93, 81.1, 80.4, 80.3 and 73.8 %, respectively. This infers that the addition of TPS and fibers had reduced the degradation ability of the PBAT/TPS films, which were conducive to light and thermal degradation. From the TGA and DTG graphs, it shows that upon the addition of SB and SBT fibers, the sample experienced significant weight loss at 280 to 350 °C, which implies the degradation of hemicellulose and pectin, while weight loss occurred at 300 to 500 °C correspond to lignin and cellulose overlapped with PBAT decomposition event (Cardoso et al., 2018). The decreased thermal decomposition of the composites could be explained by the lower decomposition temperatures of these components compared to the matrix. Similar patterns were observed in other natural fibers such as those of SB (Vera, 2019), peach palm trees (Cordeiro et al., 2017), cotton fiber (Calabia et al., 2013), and rice husk flour (Chen et al., 2015). Moreover, the functionalization of the fibers with GPTMS resulted in a slight shift of the main decomposition peak at 420 °C towards higher temperatures, indicating some improvement in thermal stability. This might be due to the formation of a refractory siloxane network after silanization (Kane et al., 2016). It is also essential to note that the TGA results indicate that both PBAT/TPS blend and composite films are thermally stable up to temperatures around 280 °C which is compatible for packaging and agricultural mulching film application.

3.4 Functional groups analysis

Figure 4 compares the FTIR spectra of the 5% untreated (SB) and treated bagasse (SBT). The spectra of both composites exhibit the main peaks at 2954 and 2850 cm^{-1}, corresponding to asymmetric and symmetric C-H stretching of the methylene (-CH$_2$-) group, respectively. Peaks at 1712, 900, and 700 cm^{-1} were associated with stretching of the ester carbonyl group (C=O), bending peaks of benzene substitute, and adjacent of methylene group (-CH$_2$-) of PBAT, respectively. Whereas the broad band at 3200 to 4000 cm^{-1} and the peaks between 1000 to 1200cm^{-1} are due to stretching of OH groups and C-O-C stretching present in the anhydroglucose ring from TPS and SB component.

From the spectrum, the change in peak at 3417cm^{-1} corresponds to the hydroxyl group from TPS component and cellulose in SB filler. The intensity of the peak increase with SBT than SB fiber indicating most of the –OH groups of the cellulose formed bonds with the silanol end group of the hydrolyzed silane. Furthermore, a tiny shoulder peak at 1120 cm^{-1} may indicate the presence of glycidylpropyl silane group in the treated SB composites. The shoulder peak's low intensity is due to the small amount of diluted GPTMS used in the SB silanization process. Similar observations also were found by Cordeiro et al. (2017), Kane et al. (2016) and Lule & Kim (2021) with GPTMS-treated peach palm tree, chitosan, and coffee husk fibers, respectively. The effect of alkaline treatment can

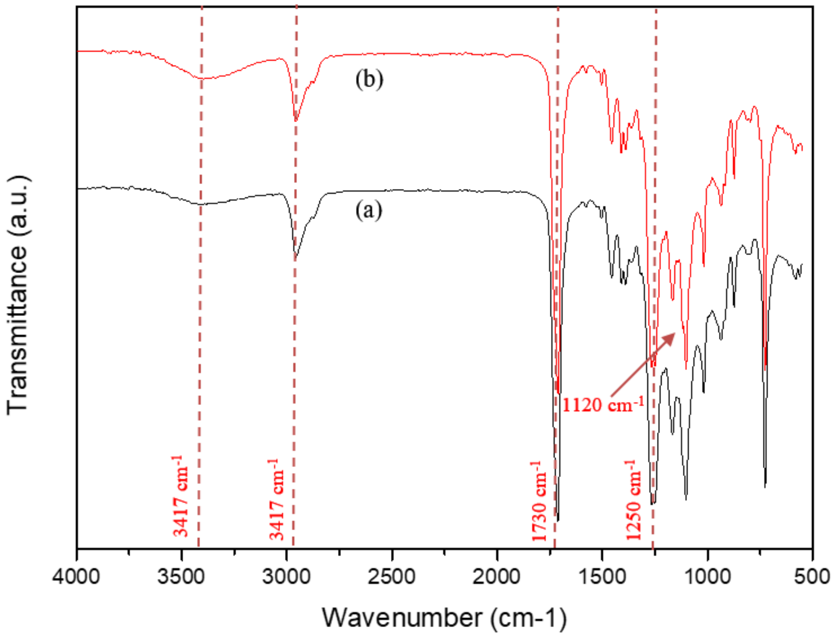

Figure 4: FTIR spectra of PBAT/TPS with 5% of (a) SB and (b) SBT fiber.

be observed by the peak weakened at 1730 and 1258 cm^{-1} of film with SBT fiber indicating partial vanishment of pectin and waxes, and hemicellulose and lignin, respectively, as previously noted by Fiorentini et al. (2022), Rout et al. (2016) and Suwan et al. (2022). This result is supported by the appearance of a rough surface of SBT fiber from the SEM images due to the removal of waxes, hemicellulose, and lignin.

3.5 Water absorption analysis

Figure 5 shows the water absorption rate of the composites. The graph shows that all films absorbed less than 8% of water after 72 hrs of testing, indicating good water barrier property. This is due to the large percentage of PBAT content in PBAT/TPS blend (90%) which has hydrophobic characteristics wrapped in the TPS and fiber particles, which are both hydrophilic.

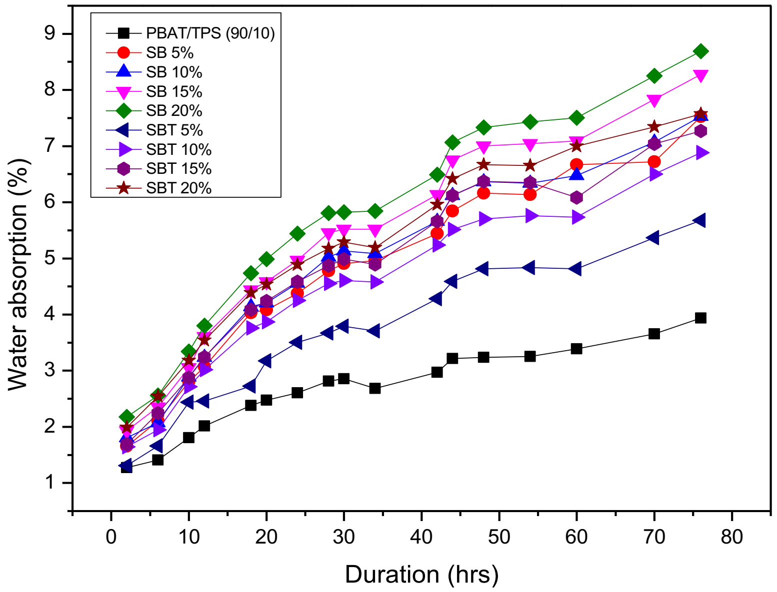

Figure 5: Water absorption rate of PBAT/TPS blend and composites.

In addition, PBAT/TPS (90/10) exhibiting the lowest water absorption rate, and increased fiber contents led to a higher water absorption rate. This might be due to the SB fiber surface contained many hydrophilic groups, which easily absorb moisture during the testing, causing swelling. Low barrier property of PBAT to water vapor also promotes this process. Additionally, the water-induced swelling of plasticized starch particles may induce surface deterioration in composite materials, facilitating water penetration and absorption by the TPS particles within the material. Consequently, higher fiber contents led to more pronounced penetration and increased water absorption in the composite. Ayu et al. (2020) and Binti Mohd Hafidz et al. (2021) also obtained similar findings upon increasing fiber loading in PBS/TPS polyester composites.

Moreover, it can also be observed that composites with alkaline and silane surface treatment by GPTMS had enhanced the water barrier properties of the films since the water absorption rate significantly decreased after surface treatment. Surface modification by silanization with hydrophobic moieties leads to improved adhesion of fiber surface to the matrix and causes less water absorbed. This result indicates that the silanization process reduces water absorption of the fibers and may give resistance against fungal decay. Furthermore, delignification by alkaline treatment also contributes to less water absorption, since lignin has an amorphous structure and is more susceptible to water absorption (Benini et al., 2011).

3.6 Contact angle (CA)

Surface hydrophobicity was determined by measuring the CA of water droplets. Table 1 summarizes CA of PBAT/TPS blend and composites. PBAT/TPS (90/10) exhibited the highest CA with 92.4°, followed by SB 5%, SB 10%, SB 15%, and SB 20%. Dispersion of hydrophilic SB fibers was expected to decrease in CA due to increased surface hydrophilicity. Furthermore, the incorporation of fiber created rougher film's surface and corresponding reduced surface energy, leading to lower CA than matrix (Wongphan et al., 2022). As expected, treated SB (SBT) fiber has improved surface hydrophobicity as the CA value is higher than untreated SB. This is due to reduced cavities between fiber surface and matrix by hydrophobic silane surface modification, creating more homogenous fiber-matrix interface and enhancing surface hydrophobicity.

Table 1: Contact angle of PBAT/TPS blend and composites

Sample	Average contact angle	
	SB	SBT
0%	92.38 ± 3.9	
5%	77.94 ± 3.5	80.46 ± 4.6
10%	74.72 ± 7.3	77.67 ± 2.1
15%	72.22 ± 6.2	73.83 ± 3.6
20%	71.10 ± 2.4	72.20 ± 3

4. CONCLUSION

In conclusion, the presented PBAT/TPS/SB composites with 5 to 15% SB fiber loadings showed adequate tensile properties (9 to 13.4 MPa), higher thermal stability (up to 280 °C), good water barrier property (less than 8% water absorption after 72 hrs) and hydrophobicity property. Furthermore, alkaline and GPTMS silane treatments had increased SB composite's tensile strength and flexibility about 6 to 15% compared to untreated SB. The effect of silane and alkaline surface treatment by GPTMS coupling agent and NaOH can be seen in the increase in fiber surface roughness and the reduction in fiber-matrix gap in SEM image for 5% SBT, indicating better interfacial adhesion than without treatment. However, at a higher bagasse filler fraction (20%), weak coupling effect can be observed, probably due to insufficient coupling agent to fully cover the surface of the fiber. Moreover, the fibers had tendency to agglomerate leading to poor wetting of hydrophilic SB filler by hydrophobic matrix.

ACKNOWLEDGMENT

The authors were grateful to the Universiti Sains Malaysia (Research University Grant No. 8014044) for the financial support and Universiti Malaysia Perlis (UniMAP) for the scholarship granted to the first author. We would also like to thank the School of Materials and Mineral Resources Engineering, Universiti Sains Malaysia (USM) for providing their facilities.

REFERENCES

Ayu, R. S., Khalina, A., Harmaen, A. S., Zaman, K., Isma, T., Liu, Q., Ilyas, R. A., & Lee, C. H. (2020). Characterization Study of Empty Fruit Bunch (EFB) Fibers Reinforcement in Poly(Butylene) Succinate (PBS)/Starch/Glycerol Composite Sheet. *Polymers*, *12*(7), 1571. https://doi.org/10.3390/polym12071571

Benini, K. C. C. C., Voorwald, H. J. C., Cioffi, M. O. H., & Al, E. (2011). Mechanical properties of HIPS/sugarcane bagasse fiber composites after accelerated weathering. *Procedia Engineering*, *10*(December), 3246–3251. https://doi.org/10.1016/j.proeng.2011.04.536

Binti Mohd Hafidz, N. S., Bin Mohamed Rehan, M. S., & Binti Mokhtar, H. (2021). Effect of alkaline treatment on water absorption and thickness swelling of natural fiber reinforced unsaturated polyester composites. *Materials Today: Proceedings*, *48*, 720–727. https://doi.org/10.1016/j.matpr.2021.02.209

Calabia, B. P., Ninomiya, F., Yagi, H., Oishi, A., Taguchi, K., Kunioka, M., & Funabashi, M. (2013). Biodegradable poly(butylene succinate) composites reinforced by cotton fiber with silane coupling agent. In *Polymers* (Vol. 5, Issue 1, pp. 128–141). https://doi.org/10.3390/polym5010128

Cardoso, M. A. P., Carvalho, G. M., Yamashita, F., Mali, S., Eiras, D., Demiate, I. M., & Grossmann, M. V. E. (2018). Oat hull fibers bleached by reactive extrusion with alkaline hydrogen peroxide in thermoplastic starch/poly(butylene adipate-co-terephthalate) composites. *Polymer Composites*, *39*(6), 1950–1958. https://doi.org/10.1002/pc.24151

Chen, R. S., Ab Ghani, M. H., Ahmad, S., Salleh, M. N., & Tarawneh, M. A. (2015). Rice husk flour biocomposites based on recycled high-density polyethylene/polyethylene terephthalate blend: Effect of high filler loading on physical, mechanical and thermal properties. *Journal of Composite Materials*, *49*(10), 1241–1253. https://doi.org/10.1177/0021998314533361

Cordeiro, E. P., Pita, V. J. R. R., & Soares, B. G. (2017). Epoxy–Fiber of Peach Palm Trees Composites: The Effect of Composition and Fiber Modification on Mechanical and Dynamic Mechanical Properties. *Journal of Polymers and the Environment*, *25*(3), 913–924. https://doi.org/10.1007/s10924-016-0841-0

De Moura, C. V. R., Da Cruz Sousa, D., De Moura, E. M., De Araújo, E. C. E., & Sittolin, I. M. (2021). New biodegradable composites from starch and fibers of the babassu coconut. *Polimeros*, *31*(1). https://doi.org/10.1590/0104-1428.09519

Fiorentini, C., Bassani, A., Duserm Garrido, G., Merino, D., Perotto, G., Athanassiou, A., Peräntie, J., Halonen, N., & Spigno, G. (2022). High-pressure autohydrolysis process of wheat straw for cellulose recovery and subsequent use in PBAT composites preparation. *Biocatalysis and Agricultural Biotechnology*, *39*(January). https://doi.org/10.1016/j.bcab.2022.102282

González Seligra, P., Eloy Moura, L., Famá, L., Druzian, J. I., & Goyanes, S. (2016). Influence of incorporation of starch nanoparticles in PBAT/TPS composite films. *Polymer International*, *65*(8), 938–945. https://doi.org/10.1002/pi.5127

Jamali, V. P., Sudagar, I., Author, C., Sudha, P., Boomiraj, K., & Naik, R. (2021). Influence of sugarcane bagasse fibers from the rind and pith on selected properties of bio-composite material. *~ 2417 ~ The Pharma Innovation Journal*, *10*(10), 2417–2422. http://www.thepharmajournal.com

Kane, S. N., Mishra, A., & Dutta, A. K. (2016). Preface: International Conference on Recent Trends in Physics (ICRTP 2016). *Journal of Physics: Conference Series*, *755*(1). https://doi.org/10.1088/1742-6596/755/1/011001

Lee, S. C., & Mariatti, M. (2008). *The effect of bagasse fibers obtained (from rind and pith component) on the properties of unsaturated polyester composites*. *62*, 2253–2256. https://doi.org/10.1016/j.matlet.2007.11.097

Lendvai, L., Apostolov, A., & Karger-Kocsis, J. (2017). Characterization of layered silicate-reinforced blends of thermoplastic starch (TPS) and poly(butylene adipate-co-terephthalate). *Carbohydrate Polymers*, *173*, 566–572. https://doi.org/10.1016/j.carbpol.2017.05.100

Liu, W., Liu, S., Wang, Z., Dai, B., Liu, J., Chen, Y., Zeng, G., He, Y., Liu, Y., & Liu, R. (2019). Preparation and characterization of reinforced starch-based composites with compatibilizer by simple extrusion. *Carbohydrate Polymers*, *223*(January), 115122. https://doi.org/10.1016/j.carbpol.2019.115122

Lule, Z. C., & Kim, J. (2021). Properties of economical and eco-friendly polybutylene adipate terephthalate composites loaded with surface treated coffee husk. *Composites Part A*, *140*(October 2020), 106154. https://doi.org/10.1016/j.compositesa.2020.106154

Nunes, M. A. B. S., Marinho, V. A. D., Falcão, G. A. M., Canedo, E. L., Bardi, M. A. G., & Carvalho, L. H. (2018). Rheological, mechanical and morphological properties of poly(butylene adipate-co-terephthalate)/thermoplastic starch blends and its biocomposite with babassu mesocarp. *Polymer Testing*, *70*(June), 281–288. https://doi.org/10.1016/j.polymertesting.2018.07.009

Pereira da Silva, J. S., Farias da Silva, J. M., Soares, B. G., & Livi, S. (2017). Fully biodegradable composites based on poly(butylene adipate-co-terephthalate)/peach palm trees fiber. *Composites Part B: Engineering*, *129*, 117–123. https://doi.org/10.1016/j.compositesb.2017.07.088

Ramlee, N. A., Jawaid, M., Zainudin, E. S., & Yamani, S. A. K. (2019). Tensile, physical and morphological properties of oil palm empty fruit bunch/sugarcane bagasse fiber reinforced phenolic hybrid composites. *Journal of Materials Research and Technology*, *8*(4), 3466–3474. https://doi.org/10.1016/j.jmrt.2019.06.016

Rout, A. K., Kar, J., Jesthi, D. K., & Sutar, A. K. (2016). Effect of surface treatment on the physical, chemical, and mechanical properties of palm tree leaf stalk fibers. *BioResources*, *11*(2), 4432–4445. https://doi.org/10.15376/biores.11.2.4432-4445

Suwan, T., Maichin, P., Fan, M., Jitsangiam, P., Tangchirapat, W., & Chindaprasirt, P. (2022). Influence of alkalinity on self-treatment process of natural fiber and properties of its geopolymeric composites. *Construction and Building Materials*, *316*(November 2021), 125817. https://doi.org/10.1016/j.conbuildmat.2021.125817

Vera, F. L. (2019). Characterizations of Some Composite Materials. *Characterizations of Some Composite Materials*, *February*. https://doi.org/10.5772/intechopen.73357

Wirawan, R., Sapuan, S. M., Abdan, K., & Yunus, R. (2011). Tensile and impact properties of sugarcane bagasse/poly (vinyl chloride) composites. *Key Engineering Materials*, *471–472*, 167–172. https://doi.org/10.4028/www.scientific.net/KEM.471-472.167

Wongphan, P., Panrong, T., & Harnkarnsujarit, N. (2022). Effect of different modified starches on physical, morphological, thermomechanical, barrier and biodegradation properties of cassava starch and polybutylene adipate terephthalate blend film. *Food Packaging and Shelf Life*, *32*(March), 100844. https://doi.org/10.1016/j.fpsl.2022.100844

Yap, S. Y., Sreekantan, S., Hassan, M., Sudesh, K., & Ong, M. T. (2020). Characterization and Biodegradability of Rice Husk-Filled Polymer Composites. *Polymers*, *13*(1), 104. https://doi.org/10.3390/polym13010104

Yokesahachart, C., Yoksan, R., Khanoonkon, N., Mohanty, A. K., & Misra, M. (2021). Effect of jute fibers on morphological characteristics and properties of thermoplastic starch/biodegradable polyester blend. *Cellulose*, *28*(9), 5513–5530. https://doi.org/10.1007/s10570-021-03921-8